bjh research paper

Analysis of human leukaemias and lymphomas using extensive immunophenotypes from an antibody microarray

Larissa Belov,[1] Stephen P. Mulligan,[2,3] Nicole Barber,[2] Adrian Woolfson,[4] Mike Scott,[5] Kerryn Stoner,[5] Jeremy S. Chrisp,[1] William A. Sewell,[6] Kenneth F. Bradstock,[7] Linda Bendall,[7] Dana S. Pascovici,[8] Mervyn Thomas,[8] Wendy Erber,[5] Pauline Huang,[1] Mary Sartor,[7] Graham A.R. Young,[9] James S. Wiley,[10] Surender Juneja,[11] William G. Wierda,[12] Anthony R. Green,[5] Michael J. Keating[12] and Richard I. Christopherson[2]

[1]Medsaic Pty Ltd, Suite 145, level1, National Innovation Centre, Australian Technology Park, Garden Street, Eveleigh, Australia, [2]School of Molecular and Microbial Biosciences, University of Sydney, Sydney, NSW, Australia, [3]Symbion Health, North Ryde, Sydney, NSW, Australia, [4]Addenbrooke's Hospital, University of Cambridge School of Clinical Medicine, Cambridge, UK, [5]Department of Haematology, Addenbrooke's Hospital, University of Cambridge, Cambridge, UK, [6]Institute of Laboratory Medicine, St Vincent's Hospital Sydney, Darlinghurst, NSW, Australia, [7]Westmead Millennium Institute, University of Sydney, Westmead, NSW, Australia, [8]Emphron Informatics Pty Ltd, Chapel Hill, Qld, Australia, [9]Kanematsu Research Laboratories, University of Sydney, NSW, Australia, [10]Department of Medicine, Nepean Hospital, Penrith, NSW, Australia, [11]Diagnostic Haematology, Melbourne Health Shared Pathology Service, Royal Melbourne Hospital, Parkville, Victoria, Australia and [12]MD Anderson Cancer Center, Houston, TX, USA

Received 28 March 2006; accepted for publication 23 June 2006

Correspondence: R.I. Christopherson, School of Molecular and Microbial Biosciences, University of Sydney, NSW 2006, Australia.
E-mail: ric@mmb.usyd.edu.au

Summary

A novel antibody microarray has been developed that provides an extensive immunophenotype of leukaemia cells. The assay is a solid phase cell-capture technique in which 82 antigens are studied simultaneously. This paper presents the analysis of 733 patients with a variety of leukaemias and lymphomas from peripheral blood and bone marrow. Discriminant Function Analysis of the expression profiles from these 733 patients and 63 normal subjects were clustered and showed high levels of consistency with diagnoses obtained using conventional clinical and laboratory criteria. The overall levels of consensus for classification using the microarray compared with established criteria were 93·9% (495/527 patients) for peripheral blood and 97·6% (201/206 patients) for bone marrow aspirates, showing that the extensive phenotype alone was frequently able to classify the disease when the leukaemic clone was the dominant cell population present. Immunophenotypes for neoplastic cells were distinguishable from normal cells when the leukaemic cell count was at least 5×10^9 cells/l in peripheral blood, or 20% of cells obtained from bone marrow aspirates. This technique may be a useful adjunct to flow cytometry and other methods when an extensive phenotype of the leukaemia cell is desired for clinical trials, research and prognostic factor analysis.

Keywords: leukaemia, CD antigens, immunophenotype, expression profile, array.

Leukaemias are currently diagnosed by a combination of morphological analysis, cytochemistry, immunophenotyping, cytogenetics and molecular genetics. The French–American–British (FAB) system divides acute myeloid leukaemia (AML) into eight subtypes (M0–M7) and acute lymphoblastic leukaemia (ALL) into three subtypes (L1–L3), for both

B- and T-cell lineages (Bennett *et al*, 1976, 1991; Bain, 2003). The World Health Organisation (WHO) classification for AML builds upon the morphological criteria used in the FAB system (Jaffe *et al*, 2001). Immunophenotypic analysis has a central role in distinguishing between minimally differentiated AML and ALL, for recognition of acute megakaryoblastic leukaemia, and in the separation of B- and T-cell ALL (Jaffe *et al*, 2001). The biphenotypic acute leukaemias, acute leukaemias with lineage infidelity, minimally differentiated AML, and some Precursor ALL can only be distinguished through immunophenotyping (Brunning, 2003). The European Group for the Immunologic Classification of Leukaemia (EGIL) proposed a scoring system to identify biphenotypic leukaemias (Bene *et al*, 1995). Relationships between immunophenotype, classification and prognosis of leukaemias have been studied extensively (Ferrara *et al*, 1998; Khalidi *et al*, 1998, 1999; Exner *et al*, 2000; Dunphy *et al*, 2001; Raspadori *et al*, 2001; Thalhammer-Scherrer *et al*, 2002; Munoz *et al*, 2003). Casasnovas *et al* (2003) developed a classification system for AML based on immunophenotypes from seven antigens, defining five subtypes, MA–ME, that correlated with prognosis. A more extensive immunophenotype should enable more accurate diagnostic and prognostic analysis.

The B-lymphoproliferative disorders (B-LPD) encompass a broad range of leukaemias and lymphomas. Distinctions between some of the B-LPD may be subtle; for example, chronic lymphocytic leukaemia (CLL) and mantle cell leukaemia (MCL) differ in the level of CD23, D1-cyclin and surface immunoglobulin expression. B-LPD have been classified by the FAB system (Bennett *et al*, 1989), and more recently by the WHO classification (Jaffe *et al*, 2001). The WHO classification divides B-LPD into subtypes that correspond to various stages of B-cell differentiation, ranging from naïve B cells to plasma cells. The B-LPD and their relationship to normal B-cell differentiation have been reviewed by Shaffer *et al* (2002); phenotype is a crucial component for diagnosis and classification of B-LPD. Some B-LPD do not correspond with classic differentiation states, for example, hairy cell leukaemia (HCL) and CLL.

Gene expression profiling may sub-cluster some leukaemias and lymphomas (Staudt, 2003). For example, DNA microarrays representing 32 275 unique Unigene clusters (Stanford Functional Genomics Facility protocol) have been used by Lacayo *et al* (2004) on samples from childhood AML patients to identify *FLT3* mutations with good clinical outcomes. However, DNA microarrays may be too complex for routine screening, and the expression of cellular proteins does not always correlate with mRNA levels. A procedure that simultaneously measures the expression of many proteins on the surface of leukaemia cells would be an important analytical tool. We have developed a cluster of differentiation (CD) antibody microarray (DotScan^{TM}) containing immobilised monoclonal antibody dots (10 nL) specific for 82 CD antigens. Leucocytes are captured by the corresponding immobilised antibody, yielding a dot pattern that defines the surface immunophenotype (expression profile, disease signature) of those cells (Belov *et al*, 2001, 2003). Several groups have proposed that extensive immunophenotyping should be sufficient to sub-classify leukaemias. Nguyen *et al* (2000) developed a relational database that included the diagnostic immunophenotypes for 33 haematopoietic neoplasms. The database included the expression of 42 CD antigens and the correct diagnosis was listed in the top 5 differential diagnoses for 89% of a panel of 92 clinical cases. It was concluded that a pathologist must establish the final diagnosis by correlating histological findings with the immunophenotype. Bain (2003) compiled a table for AML (M0–M7) that summarised patterns of reactivity for categories of AML with antibodies against CD11b, CD13, CD14, CD15, CD33, CD34, CD117, HLA-DR and TdT (intracellular). These proteins were differentially expressed between the subtypes of AML, suggesting that it might be possible to reclassify these leukaemias based upon extensive immunophenotypes. Flow cytometry has been the standard method for cell surface analysis and it remains a powerful technique particularly for leucocyte subset analysis, but its utility to provide an extensive immunophenotype is limited by cost and time. The availability of a simple, internally consistent and unbiased system for classification of all leukaemias and lymphomas would be a significant advance.

This study analysed the immunophenotypes from the peripheral blood (PB) of 29 normal subjects and 527 patients with leukaemia or lymphoma, and from bone marrow aspirates (BMA) of 34 control subjects and 206 patients. Regularised high-dimensional classification techniques were used to define cell surface antigen profiles for each leukaemia and its associated subtypes. The data obtained with the CD antibody microarray correlated closely with the diagnoses provided by 'traditional' methods, including flow cytometric immunophenotyping, validating the use of this microarray for clinical diagnosis, and opening the possibility for further dissecting the biological and clinical heterogeneity of human leukaemias and lymphomas.

Materials and methods

CD antibody microarrays

Medsaic Pty Ltd (Eveleigh, NSW, Australia) provided the DotScan^{TM} microarrays, prepared as previously described (Belov *et al*, 2001). Monoclonal antibodies were purchased from the following companies: Coulter and Immunotech from Beckman Coulter (Gladesville, NSW, Australia), Pharmingen from BD Biosciences (North Ryde, NSW, Australia), Biosource International from Applied Medical (Stafford City, Qld, Australia), Serotec from Australian Laboratory Services (Sydney Markets, NSW, Australia), Sigma-Aldrich (Castle Hill, NSW, Australia), Biotrend, Biodesign and MBL from Jomar Diagnostics (Stepney, SA, Australia), Chemicon Australia (Boronia, Vic., Australia) and Leinco Technologies (St Louis, MO, USA) and Calbiochem from Merck (Kilsyth, Vic., Australia). Antibody solutions were reconstituted as

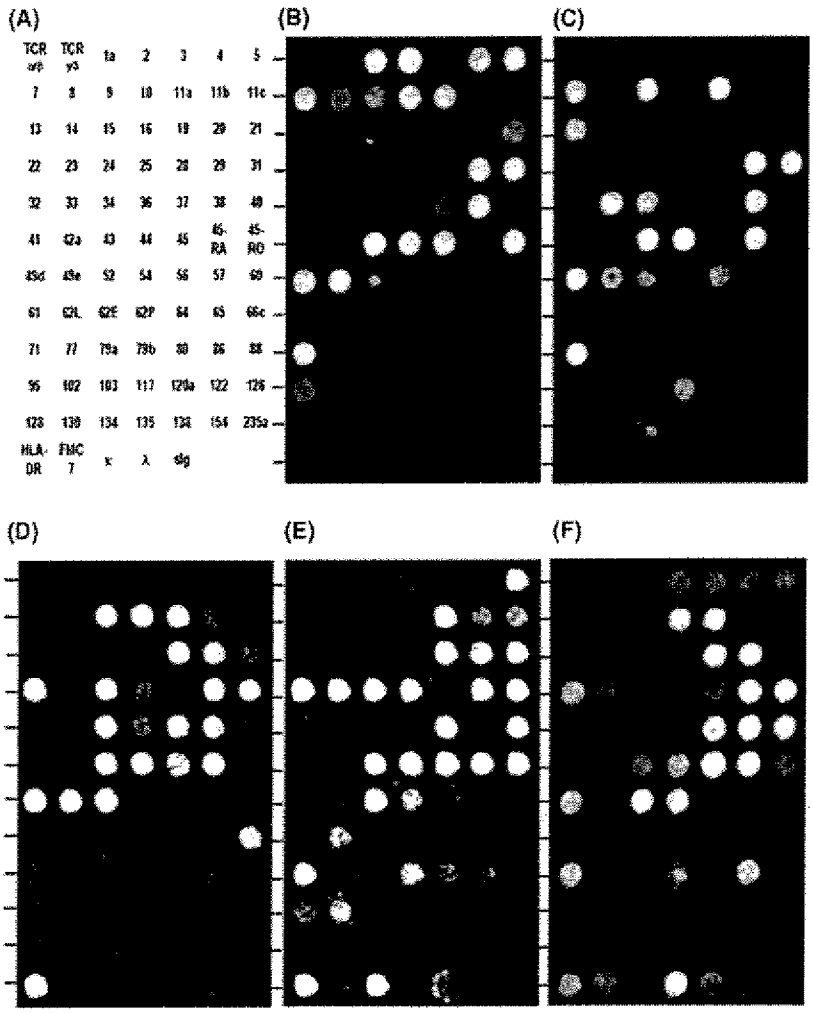

Fig 1. Representative dot patterns for leukaemia cells captured on CD antibody microarrays. (A) Key; (B) T-ALL-63772; (C) AML-87878; (D) Precursor B-379; (E) B-CLL-382; (F) FL-86065. The numbers in the key refer to positions of CD antibodies; TCRα/β and TCRγ/δ are T-cell receptors, HLA-DR, FMC7, κ and λ are immunoglobulin light chains, and sIg is surface immunoglobulin. Samples from patients are identified by their abbreviated disease name followed by the assay code number. Leucocytes did not bind to the murine isotype control antibodies, mIgG1, mIgG2a, mIgG2b and mIgM (not shown). Details of the fractionation of mononuclear leucocytes and immunophenotyping with CD antibody microarrays appear in *Materials and methods*. The intensities of the dots in these patterns were quantified as described in *Materials and methods* and are presented in Table I with corresponding flow cytometric data.

recommended, and stored in aliquots with 0·1% (w/v) bovine serum albumin (BSA) at −80°C, Pharmingen antibodies were generally stored at 4°C with BSA added to 0·1% (w/v) before dispensing. Antibodies were used for making microarrays at concentrations ranging from 50 to 1000 μg protein/ml.

Immunophenotyping leucocytes from patients

After obtaining informed consent, blood (5 ml) or bone marrow (1 ml) was collected from patients by venepuncture or needle aspiration into a tube containing heparin or EDTA. The project received approval from the Human Research Ethics Committee at Royal Prince Alfred Hospital (Camperdown, NSW, Australia; permit no. 99/07/07), and the Human Research Ethics Committee of St Vincent's Hospital (Darlinghurst, NSW, Australia; reference number H02/074). Blood samples were obtained from Symbion Pathology (North Ryde, NSW, Australia), Westmead Millennium Institute (Westmead Hospital, Westmead, NSW, Australia), Garvan Institute of Medical Research (Darlinghurst, NSW, Australia), University of Cambridge Department of Haematology (Addenbrooke's Hospital, Cambridge, UK), MD Anderson Cancer Center, (Houston, TX, USA), Diagnostic Haematology, Melbourne Health Shared Pathology Service, Royal Melbourne Hospital (Parkville, Vic., Australia), Kanematsu Research Laboratories (University of Sydney, NSW, Australia), and the Department of Medicine (Nepean Hospital, Penrith, NSW, Australia). Most blood samples were analysed within 48 h; approximately 20%

of samples were obtained as mononuclear leucocytes frozen in a viable state in dimethyl sulphoxide/fetal calf serum using established procedures. Control experiments have shown that frozen viable cells, when thawed, give a similar immunophenotype to a fresh sample (Belov *et al*, 2003). Total leukaemic cell counts in the samples analysed varied from 4·0–200 × 10^9/l. Most of the bone marrow samples were obtained from the Garvan Institute of Medical Research (Darlinghurst, NSW, Australia); leukaemic cells accounted for at least 10% of marrow leucocytes. The project described in this paper was approved by all of the above institutions that supplied samples.

Mononuclear leucocytes were obtained and analysed from blood and bone marrow samples as previously described (Belov *et al*, 2003). Briefly, a 300 μl aliquot of the leucocyte suspension (4×10^6 cells) was incubated for 30 min on the microarray, then unbound cells were removed by gentle washing. Captured cells were fixed and imaged using DotReader™ and dot intensities were quantified for each antigen in duplicate, using data analysis software on an 8-bit pixel greyness scale from 0 to 255 that reflected the level of expression of a particular antigen and the proportion of cells expressing that antigen (Belov *et al*, 2003). The dot pattern obtained is the immunophenotype of that population of leucocytes; immunophenotypes for neoplastic cells were distinguishable from normal cells when the leukaemic count was at least 5×10^9 cells/l in peripheral blood, or 20% of cells obtained from BMA. As the leukaemic cell count decreases, the binding pattern reflects the increasing proportion of normal leucocytes, until the clonal population is diluted below the limit of detection.

Signature expression profiles

All computations were performed using the R statistical language environment (R Development Core Team, 2005).

Table I. Comparison of immunophenotypic data from CD antibody microarrays and flow cytometry for analysis of the leukaemia samples in Fig 1.

	T-ALL-63772		AML-87878		Precursor B-379		B-CLL-382		FL-86065	
Antigen	FC	DotScan	FC	DotScan	FC	DotScan	FC	DotScan	FC	DotScan
CD2	92	100·0	3	2·0		2·8		8·1		30·9
CD3		0·9	0	1·0		3·5		3·7	35	27·1
CD4	90	82·4		0·7		1·4		3·1	28	19·5
CD5		90·6		1·5	5	2·5	97	90·7	44	25·5
CD7	92	79·2	98	78·3		2·8		3·8		17·8
CD8	36	34·9		0·8		1·3		1·4	7	1·5
CD10	25	78·0	25	5·2	79	91·7		0·8	63	84·2
CD11c		0·6		0·7		0·8		57·8		0·7
CD13	4	0·6	9	69·4	1	0·8		0·6		0·7
CD14	0	0·6	0	0·7		0·9		0·7		0·7
CD15		2·1		1·2		1·9		1·1		0·8
CD16		1·3		1·3		1·2		1·3	0	0·7
CD19	6	0·9	0	1·5	79	91·7	91	92·5	69	84·9
CD20		0·6		0·7	65	81·2	92	87·6	70	81·6
CD22		0·6		1·6		99·2		90·7	69	86·2
CD23		0·6		0·8		0·9		87·0	29	29·9
CD25		1·6		1·1		12·6		83·2		4·8
CD33	2	0·6	98	100·0	15	0·9		1·7		0·1
CD34	0	0·6	87	81·8	82	80·5		1		0·0
CD38		88·7		90·9		76·7	2	1·2		110·5
CD45	99	88·1		3·1	99	76·7		100·0		122·4
CD45RA		1·6		90·2		100		90·1		111·2
CD45RO		95·0		3·6		3·1		96·9		33·0
CD56	2	0·8	71	52·0		0·8		1·4		0·7
CD65		0·6		0·8	2	0·8		1·3		0·7
CD103		1·5		0·7		0·9		0·8		0·7
CD117	0	1·5	28	66·1	0	0·8		0·7		0·7
HLA-DR	9	0·6	2	0·8	96	96·2		83·2		77·0
FMC7		0·6		0·7		1·6		3·6		46·6
Kappa		0·9		0·8	15	1·5	91	86·3	3	0·7
Lambda		1·5		1·4	7	1·4	0	0·9	69	94·7

Microarray (DotScan™) data are presented as a percentage of the maximum intensity of 100%, while flow cytometry (FC) results are presented as percentage of a gated population (lymphocytes and/or blast cells).

The immunophenotypes of 556 PB samples and 240 BMA were grouped according to a hierarchical model for classification of leukaemias and lymphomas. Signature expression profiles, plotted as bar charts, were generated for each classification of leukaemia/lymphoma analysed, showing average cell binding intensities for the 82 surface antigens. Each bar chart was scaled to occupy the full 0–255 greyness scale. The data for the signature expression profiles, means and standard errors, have been provided as Supplementary Material (Tables S1 and S2).

The dot patterns (e.g. Fig 1) were used to predict the classification of leukaemias by using cross-validated regularised quadratic discriminant analysis. This statistical method of classification can be Bayes optimal (Venables & Ripley, 2002) under certain conditions of the data distribution (e.g. when the multivariate data are normally distributed). Regularised quadratic discriminant analysis (Friedman, 1989) incorporates two further shrinkage parameters that allow for more flexibility when modelling the data distribution. The number of parameters is kept low to avoid over-training. As in all statistical classification methods, the expression profiles of the various samples are used to train the statistical classification algorithm, and thus to generate specific signatures for each leukaemia category. The algorithm uses 'leave one out cross-validation'; all observations were used to train the classifier and all observations were used to test the classifier *but* no observation was used to train and test the classifier at the same time, ensuring that the predictions were not over-optimistic. Cross-validated quadratic discriminant analysis was carried out for each disease category and the results expressed as classification consensus, i.e. clinical diagnosis (defined as reported by the diagnostic pathology laboratory or haematologist) *versus* DotScan™ microarray diagnosis.

Classification score

Graphical displays of the results of comparisons between two disease categories were obtained using a reduced-space generalised linear model. The generalised linear model was applied to a low-dimensional summary of the antibody results for each assay (based on principal component scores). These principal component scores were used to generate the linear predictor in a binomial error model with logit link function (Venables & Ripley, 2002). For new observations (i.e. observations not used in fitting the generalised linear model), predicted values were generated on the link scale (McCullagh & Nelder, 1999), translated such that the prediction boundary between groups was at zero. Throughout this paper, these predicted values on the logit scale are referred to as classification scores. A classification score greater than zero implies predicted membership of one disease group; whilst a classification score less than zero implies predicted membership of the other disease group. The calculation of classification scores is summarised in Appendix S1.

Discriminant functions analysis

The immunophenotypic data are highly multi-dimensional, and to assist visualisation were projected onto an appropriate three-dimensional space that provided the best separation. There are several ways in which this projection can be made. The first is principal component analysis that projects the data along the directions showing maximum variance. Another option is linear discriminant analysis, where directions are chosen to maximise between-group separation. For high dimensional data, it is preferable to perform principal component analysis first utilising a large number of components ($n = 15$ components were chosen for the immunophenotypic data), followed by a discriminant analysis that improves separation. The immunophenotypic data were visualised by projection onto the space of the first three discriminant functions. After the three-dimensional projections were chosen, they were rotated and inspected manually, and the two-dimensional snapshots that presented the best separations were selected. In the case of those immunophenotypes that clustered, we concluded that the samples belonged to the same disease category and they were compared with their clinical diagnoses.

Signature tightness indicators

The disease classification algorithm relies on spatial information on the location and shape of the disease cluster that is provided by the centroid of the cluster and the variance-covariance matrix. The mean Euclidean Distance to the centroid (E) was calculated from the log-normalised cell binding intensity data, for each disease category. E is the average distance from each assay to the centroid of the respective disease cluster, a simple measure of the size of the cluster. A large value for E corresponds to a more spread-out cluster.

Fig 2. Expression profiles for acute leukaemias. (A) peripheral blood; (B) bone marrow aspirates. Leukaemias are denoted by acronyms defined in the text; numbers of patient samples tested are in brackets. The bar charts have been scaled to give a maximum intensity value of 255 on the 8-bit greyness scale as described in *Materials and methods*. The staggered numbers on the abscissa refer to CD antigens; their abbreviations are defined in the legend to Fig 1. Signature tightness expressed as values for the mean Euclidean Distance to the centroid (E) for the cluster of dot patterns for each clinical subtype were for (A) PB: Normal, 7·00; AML, 9·78; Precursor-B-ALL, 9·03; T-ALL, 9·93. (B) BMA: Control, 6·40; AML, 9·72; Precursor-B-ALL, 8·48; T-ALL, 8·53.

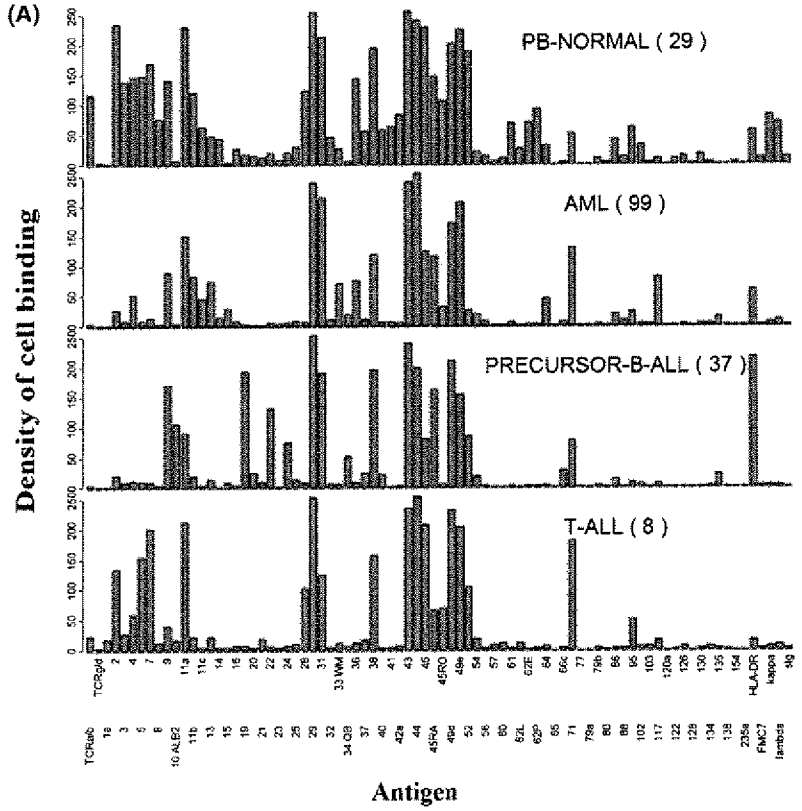

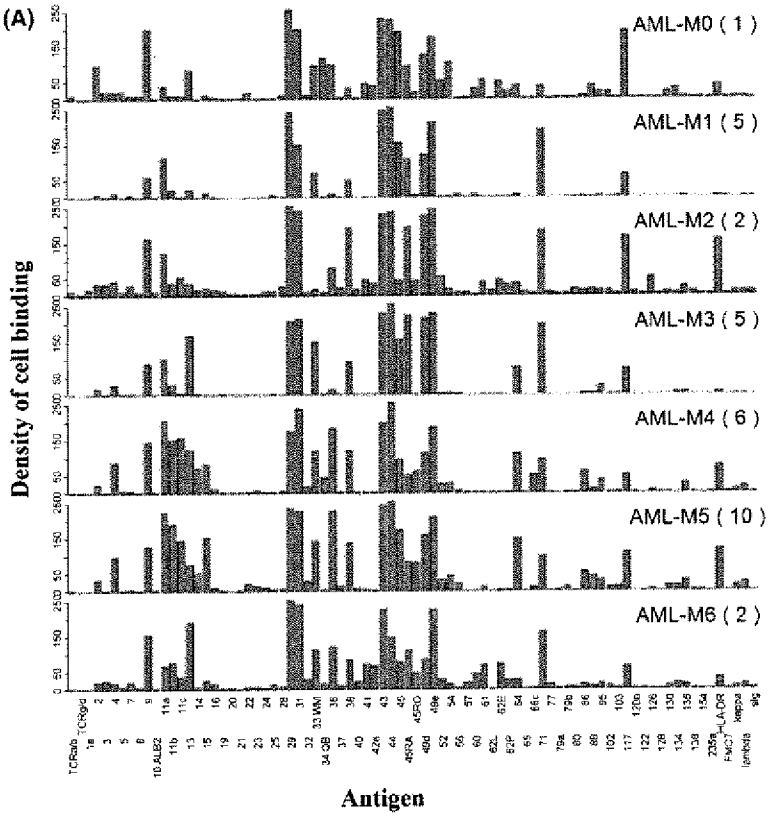

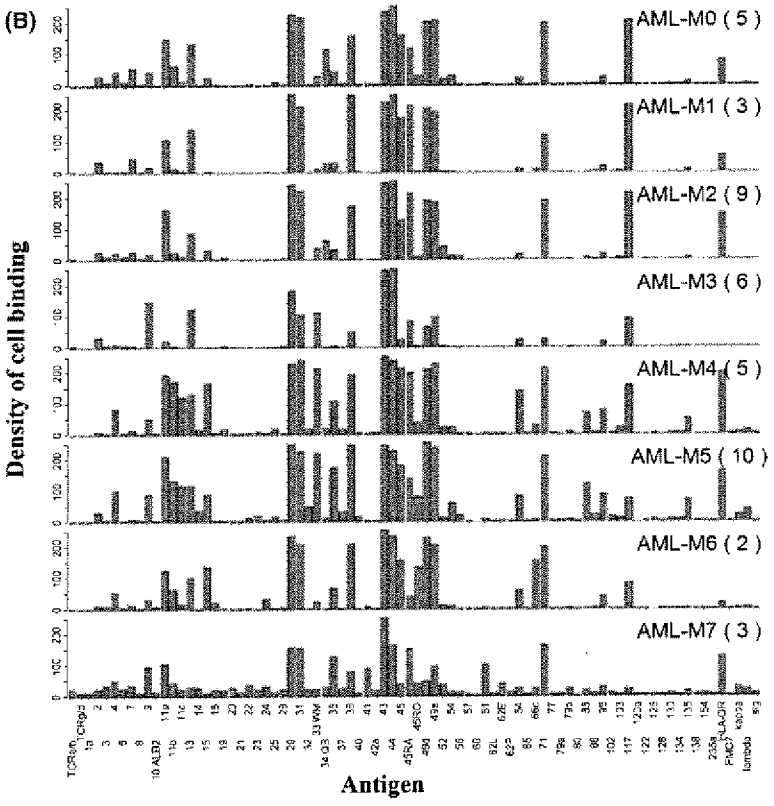

Results

Dot patterns for leukaemias

Mononuclear leucocytes from leukaemia patients, diagnosed using established criteria, were immunophenotyped using the CD antibody microarray. Examples of dot patterns are shown in Fig 1: T-ALL (Fig 1B), AML (Fig 1C), Precursor B-ALL (Precursor B, Fig 1D), B-CLL (Fig 1E), and follicular lymphoma (Fig 1F). Each of these B-cell neoplasms strongly expressed the B-cell antigens CD19 and CD20, but expression of other B-cell antigens (CD21, CD22, CD23, CD79b and immunoglobulin light chains) was variable. Table I compares DotScan™ values (expressed as a percentage of the most intense dot on the microarray) with flow cytometric data for the same patient obtained from a pathology laboratory. The data available from flow cytometry were limited by the use of time and reagents, but the data tabulated for particular CD antigens showed very good correspondence between the level of positivity from flow cytometry and the corresponding intensity percentage from the antibody microarray.

Expression profiles for acute leukaemias and B-lymphoproliferative disorders

A comparison of the average expression profiles for Histopaque-prepared PB-Normal ($n = 29$) and BMA-Control ($n = 34$) samples (Fig 2A and B) showed that the PB-Normal population expressed antigens predominantly associated with T cells (TCRα/β, CD2, CD3, CD4, CD5, CD7 and CD28), with low levels of B cell (CD19-CD23, kappa, lambda), platelet (CD41, CD42a, CD61) and myeloid (CD13, CD14 and CD33) antigens, while the BMA-control samples showed mainly immature granulocyte antigens (CD13, CD15, CD16, CD24, CD43, CD45RO and CD66c), with relatively low levels of T- and B-cell antigens. Expression of CD11a, CD31, CD43, CD44 and CD45 was high (cell binding density > 100) in both populations; CD9, CD29, CD36, CD45RA, CD49d, CD49e and CD52 were higher in PB, while CD11b and CD45RO were higher in BMA. These results reflect the normal mix of cell lineages seen in blood and marrow samples.

The average expression profile for AML samples from the PB ($n = 99$) was similar to that of BMA ($n = 112$, Fig 2A and B), with high expression of CD11a, CD29, CD31, CD38, CD43, CD44, CD45, CD45RA, CD49d, CD49e and CD71, and lower expression (cell binding density 20–100) of CD2, CD4, CD9, CD11b, CD11c, CD13, CD15, CD33, CD36, CD45RO, CD52, CD64 and HLA-DR. The average expression of CD117 was higher in AML samples taken from BMA than PB. Profiles for Precursor B-ALL samples from the PB ($n = 37$) and BMA ($n = 65$) were also comparable (Fig 2A and B), with high expression of CD9, CD10, CD19, CD22, CD29, CD31, CD38, CD43, CD44, CD45RA, CD49d, CD49e and HLA-DR, and lower expression of CD11a, CD24, CD45, CD52, CD66c and CD71. The average expression of CD34 was higher in BMA than PB. Profiles for T-ALL samples from the PB ($n = 8$) and BMA ($n = 9$) were comparable (Fig 2A and B), showing high expression of CD5, CD7, CD11a, CD29, CD31, CD38, CD43, CD44, CD45, CD49d, CD49e and CD71 and lower expression of CD4 and CD95.

Fig 3 shows expression profiles for AML cases with assigned M0–M7 subtypes from PB ($n = 31$; Fig 3A) and BMA ($n = 43$; Fig 3B). The profiles for PB and BMA were similar for a given subtype of AML. Alignment of profiles for different subtypes from PB or BMA showed differential expression of CD antigens. The expression profile for M3 AML corresponds well with reported immunophenotypes, showing little or no expression of CD11b, CD11c, CD15, CD34, CD45RO, CD86 and HLA-DR, and overexpression of CD9 (Miyachi *et al*, 1999; Re *et al*, 2002; Paietta *et al*, 2004). AML M4 and M5 expressed CD4, CD11b, CD11c, CD15, CD36, CD64 and CD86 (Brouwer *et al*, 2000; Legrand *et al*, 2000; Dunphy *et al*, 2004). CD4, CD15 and CD36 were expressed by AML M6. AML M7 expressed the megakaryocytic antigens CD9, CD41 and CD61 (Paredes-Aguilera *et al*, 2003; Yatomi *et al*, 2004), HLA-DR and CD36 (Khalidi *et al*, 1998). CD13, CD33 and CD117 contributed to the profiles of all subtypes of AML (M0–M7, Legrand *et al*, 2000). HLA-DR contributed to the profiles of all subtypes of AML except for M3 (Legrand *et al*, 2000).

Peripheral blood samples from a range of B-LPD (Fig 4A) including B-CLL ($n = 313$), follicular lymphoma (FL; $n = 3$), HCL ($n = 8$), MCL ($n = 10$) and non-Hodgkin lymphoma (NHL) of unclassified subtype ($n = 23$), showed strong expression of CD19, CD22, CD29, CD31, CD37, CD40, CD44, CD45, CD45RA, CD52 and HLA-DR, while CD9, CD54 and FMC7 were relatively low. Several antigens were differentially expressed: CD5 (B-CLL and MCL), CD23, CD43 (high in B-CLL), CD10 and CD38 (high in FL), CD11b (MCL), CD11c (HCL), CD49d (low in B-CLL), CD79b (high in FL), CD103 (HCL) and sIg (high in FL, MCL, NHL).

The NHL category includes different subtypes with peripheral blood or bone marrow involvement. Many of these individuals did not have contemporaneous nodal histology available and therefore the 'signature' for NHL does not define a single disease entity, but is a composite pattern for a range of B-LPD excluding CLL, HCL and prolymphocytic leukaemia (PLL). The expression profiles of B-CLL ($n = 11$), FL ($n = 1$) and NHL ($n = 8$) from BMA (Fig 4B) were similar to those of

Fig 3. Expression profiles of subtypes of AML. (A) peripheral blood; (B) bone marrow aspirates. The bar charts were compiled and scaled as for Fig 2 using samples classified by the FAB system for subtypes of AML (M0–M7); numbers of samples are in brackets. Signature tightness expressed as values for the mean Euclidean Distance to the centroid (E) for the cluster of dot patterns for each clinical subtype were for (A) PB: AML M0, no value; AML M1, 6·43; AML M2, 12·7; AML M3, 6·27; AML M4, 8·04; AML M5, 8·19; AML M6, 7·30. (A) BMA: AML M0, 7·57; AML M1, 6·14; AML M2, 7·67; AML M3, 6·14; AML M4, 10·6; AML M5, 10·2; AML M6, 4·50; AML M7, 4·92.

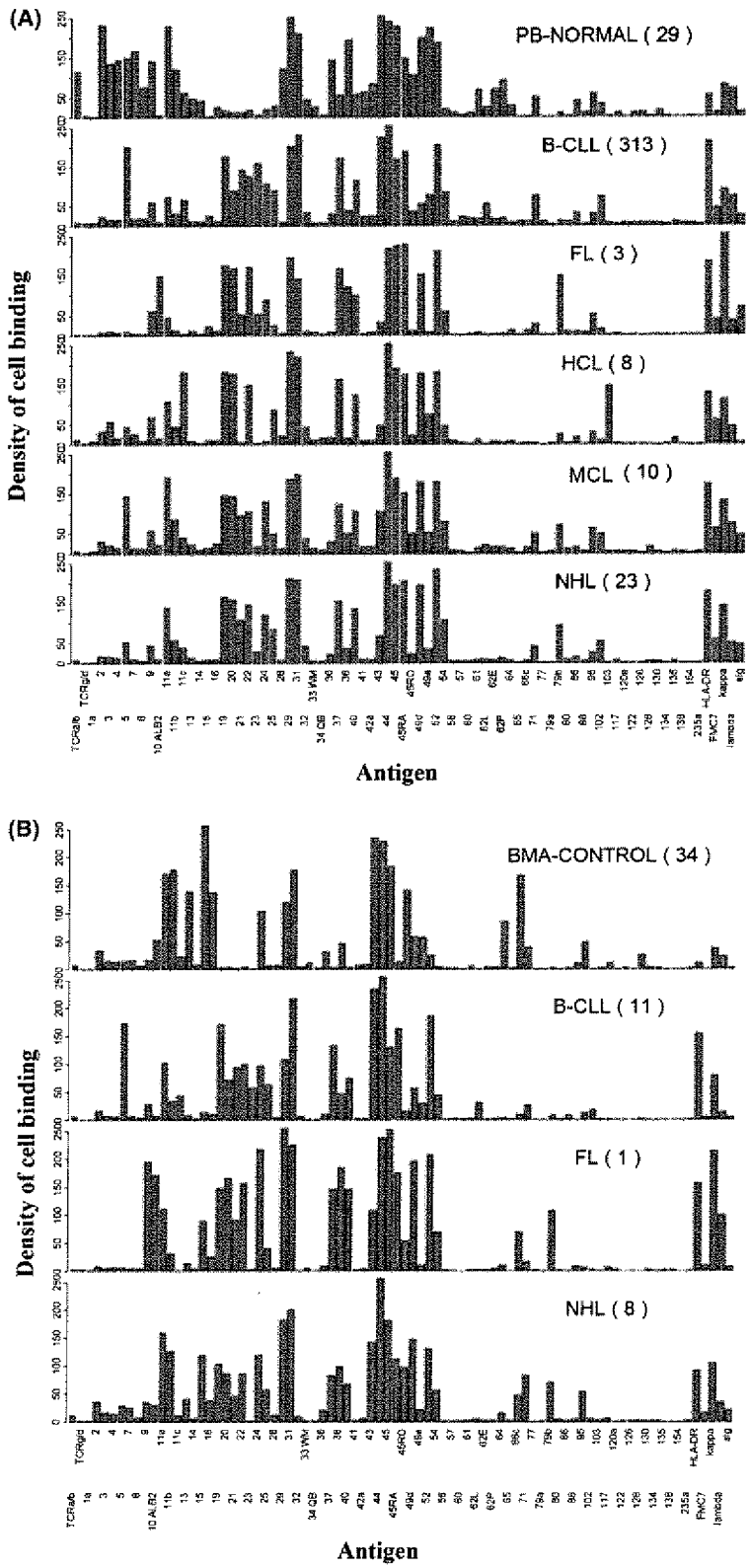

Fig 4. Expression profiles for B-lymphoproliferative disorders. (A) Peripheral blood; (B) bone marrow aspirates. The bar charts were compiled as for Fig 2. Signature tightness expressed as values for the mean Euclidean Distance to the centroid (E) for the cluster of dot patterns for each clinical subtype were for (A) PB: Normal, 7·00; B-CLL, 8·74; FL, 6·61; HCL, 7·99; MCL, 9·04; NHL, 10·3. (B) BMA: Control, 6·40; B-CLL, 8·23; FL, no value; NHL, 7·68.

PB. The striking depth and complexity of the data may potentially enable further sub-classification of leukaemias and lymphomas using cell surface expression profiles alone.

Use of classification scores to determine the threshold of detection for CLL

A model system was developed to determine the threshold proportion of CLL cells from PB that provide a distinctive dot pattern (disease signature) enabling the correct diagnosis to be made. A series of dilutions of CLL cells was prepared in a suspension of normal mononuclear leucocytes with the same total cell density ($1{\cdot}3 \times 10^7$ cells/ml). A classification score based on a reduced space linear model was used for CLL *versus* normal samples derived from the entire database. This classifier was then used to predict whether each dilution was CLL or normal peripheral blood leucocytes. The classification was derived as described above (from the logit scale-predicted values obtained with the generalised linear model). More extreme values of the score statistic provided more evidence in favour of one of the categories (CLL/normal). The value of the classification score was plotted against the known mixing proportion. Four plots are shown in Fig 5 for CLL cells from four patients. The plots are linear and showed a threshold for detection of the CLL dot pattern that varied from 0·08 to 0·23 CLL cells of the suspensions. Thus, a threshold of 20% leukaemic cells was a minimal threshold for detection of a CLL dot pattern against a background of normal mononuclear leucocytes. A conservative threshold would be 5×10^9/l leukaemia cells against a normal background of $3{\cdot}6 \times 10^9$/l total normal leucocytes.

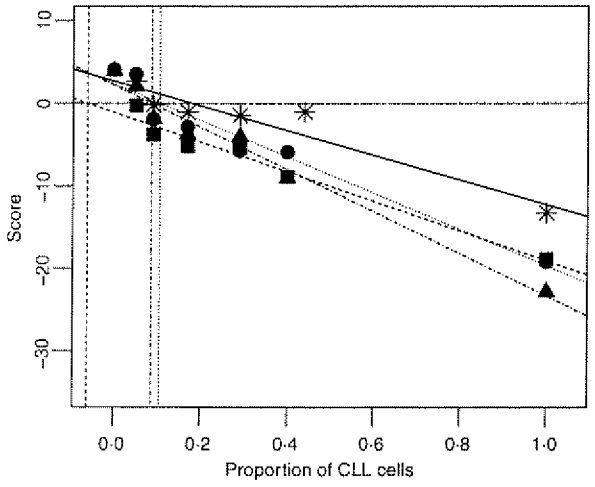

Fig 5. Classification scores for chronic lymphocytic leukaemia (CLL) as a function of the proportion of CLL cells in mononuclear leucocytes. CLL cells were taken from four patients (■, CLL1; *, CLL2; ▲, CLL3; and ●, CLL4) and purified by Histopaque centrifugation. Dilutions of the CLL cells were prepared by mixing them in the indicated proportions with normal mononuclear leucocytes from peripheral blood to give the same total cell density of $1{\cdot}3 \times 10^7$ cells/ml, and 300 μl of each suspension (4×10^6 cells) was immunophenotyped using the CD antibody microarray. Dot patterns for captured cells were recorded and classification scores calculated for each dilution as described in *Materials and methods*. The coefficient of determination (R^2) values for the linear regression fits to the data were CLL1, 0·979; CLL2, 0·983; CLL3, 0·996; CLL4, 0·982.

Correlation between clinical diagnoses and statistical clustering

Plots of discriminant function analysis for 330 acute leukaemias ($n = 144$ from PB; $n = 186$ from BMA; Fig 6) showed distinct clusters of expression profiles that corresponded with the clinical diagnoses for AML ($n = 99$ from PB; $n = 112$ from BMA), Precursor B-ALL ($n = 37$ from PB; $n = 65$ from BMA) and T-ALL ($n = 8$ from PB; $n = 9$ from BMA). These leukaemia clusters were distinct from each other and normal PB leucocytes (PB-Normal; $n = 29$) and control bone marrow

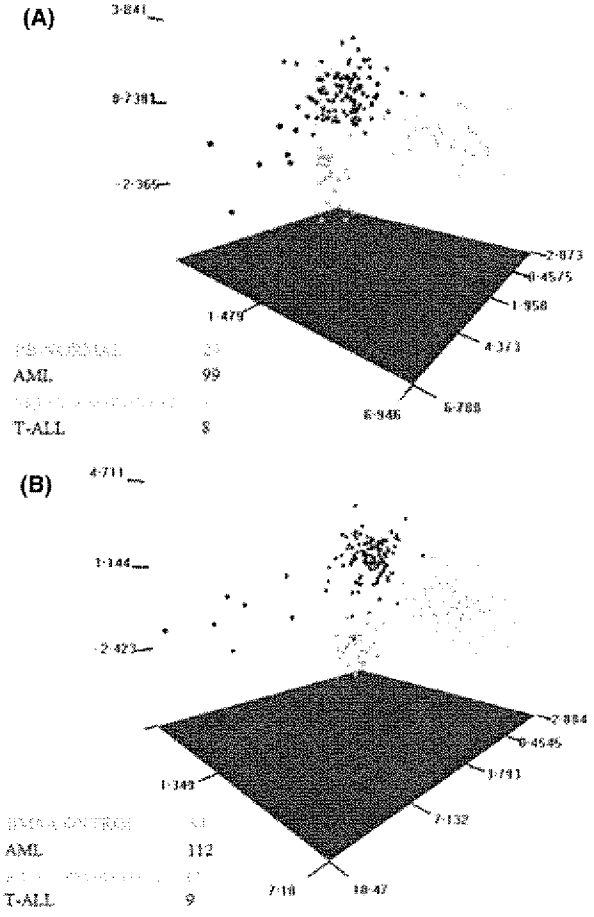

Fig 6. Discriminant function analysis plot for acute leukaemias. (A) peripheral blood; (B) bone marrow aspirates. Symbols denoting each leukaemia and the numbers of samples tested are shown with the plot. The three axes represent scores in the principal component or discriminant component space and are the first, second and third principal component. The axes do not relate directly to the usual cell binding intensities and are dimension-less.

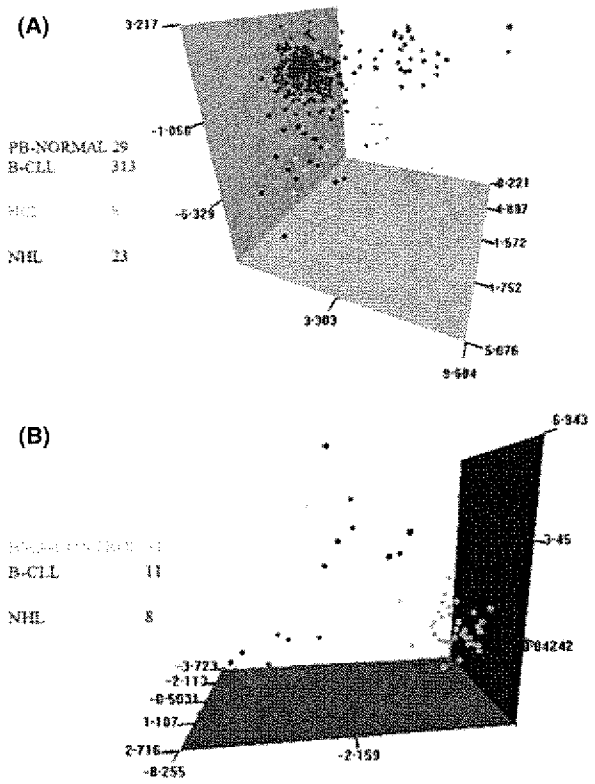

Fig 7. Discriminant function analysis plot for B-lymphoproliferative disorders. (A) Peripheral blood; (B) bone marrow aspirates. Symbols denoting each leukaemia and the numbers of samples tested are shown with the plot.

aspirates (BMA-Control; $n = 34$). Thus, the microarray was able to distinguish between these types of acute leukaemia. A similar analysis of 357 B-LPD from PB showed distinct clusters of 313 B-CLL and 29 PB-Normal, with the less numerous B-LPD in overlapping groups (Fig 7A). These subtypes of B-LPD: FL ($n = 3$), HCL ($n = 8$), MCL ($n = 10$) and NHL ($n = 23$), clustered in the three-dimensional space of the analysis, with some overlap of the mixed NHL group with MCL and FL (Fig 4). More patient data would define these profiles with greater precision. Discriminant function analysis of BMA samples of B-CLL ($n = 11$), NHL ($n = 8$), FL ($n = 1$) and BMA-Controls ($n = 34$) also showed distinct clusters (Fig 7B).

Determination of classification consensus

A total of 796 samples (556 PB and 240 BMA) were analysed using the quadratic regularised discriminant analysis for classification consensus, based solely upon an extensive immunophenotype and compared with the clinical diagnosis provided by individual institutions (*Materials and methods*). The consensus rate for PB was high (96·6–100%) for most of the disease categories (PB-Normal, AML, B-CLL, HCL and Precursor B-ALL, data not shown). That is, the microarray classification agreed with the diagnosis by pathology laboratories using conventional criteria. T-cell leukaemias were distinguished from normal samples and other disease categories in 88·2% of PB samples. However, 50% of T-ALL clustered with mature T-LPD, while 15·4% of mature T-LPD clustered with T-ALL, suggesting that intracellular TdT detection may be required to conclusively distinguish between these two categories, or alternatively, discriminatory disease signatures may be defined from extensive immunophenotypes when larger numbers of samples are analysed in each category. A few leukaemia samples clustered with PB-Normal or BMA-Control because their immunophenotypes were masked by a predominantly normal population of cells. Detection of abnormal cells became progressively more difficult when the leukaemic population was below 5×10^9 cells/l in PB or <20% of cells in BMA. In other cases, discordance could be attributed to lineage infidelity, sample quality or to small numbers of patients rather than to the performance of the assay.

Discriminatory antibodies and signature tightness

Antibodies in the microarray were ranked for discrimination between diseases. The overall ranking of the antibodies on the microarray was generated by means of a single factor analysis of variance (ANOVA) of the log-normalised cell binding intensity data for each antibody. The effectiveness of an antibody in separating all the respective disease categories included in an analysis was evaluated by the standard F-statistic, defined as the ratio of the mean square between groups (disease categories) and the mean square within groups. The associated *P*-value measuring the level of significance was also computed for each particular antibody. For PB, all 82 antibodies contributed significantly to the discrimination of diseases ($P < 0{\cdot}0005$). For BMA, 60 of 82 antibodies were significantly discriminatory ($P \leq 0{\cdot}05$). The high proportion of CD antibodies that discriminated between the subtypes of leukaemias and lymphomas was not surprising, since they were selected from many publications describing expression of CD antigens on leukaemias.

Signature tightness expressed as values for the mean Euclidean Distance to the centroid (E) for the cluster of dot patterns for each clinical subtype (listed in legends to Figs 2–4) were higher for clusters of dot patterns that showed significant variation. Values of >9·0 were obtained for PB samples of AML (9·78), Precursor-B-ALL (9·03), T-ALL (9·93), MCL (9·04), NHL (10·3), and AML M2 (12·7), compared with normals (7·00). The higher values indicated heterogeneity in the dot patterns for these diseases and either the need for more samples to define the signature (expression profile), or the potential for sub-classification of the clinical disease entity. The latter alternative is certainly true for AML, T-ALL and NHL.

Discussion

Leukaemias and lymphomas are currently diagnosed using criteria that encompass morphology, immunophenotypic

analysis, cytochemistry and cytogenetics. Development of diagnostic criteria based solely on extensive immunophenotypes has been limited by the multiple assays required using flow cytometry. The CD antibody microarray enables populations of mononuclear leucocytes to be screened using a large panel of antibodies in one assay. Results presented here show that the microarray distinguished the major categories of haematological neoplasms with high accuracy when those cells were above a threshold relative to normal cells (5×10^9 cells/l for PB, and 20% of cells in BMA). Comparison of the expression profiles of CD antigens of unknown samples with stored consensus signatures defines subtypes of acute leukaemias (AML, B-ALL and T-ALL; Fig 2), and B-LPD (B-CLL, HCL and NHL including FL and MCL; Fig 4).

There are many immunophenotypic differences between the acute leukaemias (Fig 2). The lineage discriminatory AML antigens are CD11b, CD11c, CD13, CD15, CD33, CD36, CD64 and CD117; the Precursor B antigens are CD10, CD19, CD22, CD24, CD66c and HLA-DR; the T-ALL antigens are CD2, CD5, CD7 and CD28. Immunophenotypic differences within a classification may aid in defining subtypes from a larger database. AML is especially diverse, and extensive immunophenotypes obtained with the CD antibody microarray may provide the basis for reclassification of subtypes and provide correlations for prognosis and treatment. Although the expression profiles shown in Fig 3 indicate differential expression of a number of antigens in the AML subtypes M0–M7, antigen expression may vary within each subtype.

The diagnosis of CLL is currently based on a lymphocytosis of $>5 \times 10^9$/l, and a characteristic lymphocyte morphology and immunophenotype (Oscier *et al*, 2004). CLL typically expresses CD5, CD19, CD23 and weak monotypic surface immunoglobulin (sIg), CD20 of variable intensity, while CD22, CD79b and FMC7 are often weakly expressed or absent (Jaffe *et al*, 2001; Bain, 2003; Oscier *et al*, 2004; Fig 4). This immunophenotype is consistent with data from the microarray. Differences in the expression profiles of B-LPD (see Fig 4) suggest that the CD antibody microarray can distinguish HCL and NHL (including FL and MCL) from B-CLL, although more data are required to define consensus immunophenotypes. Stable and progressive CLL may be identified by a variety of prognostic factors, such as clinical stage, mutational status of the immunoglobulin variable heavy chain gene (IgV_H), cytoplasmic Zap-70 and surface CD38 expression. We are currently correlating microarray phenotypes within B-CLL patient groups that have full prognostic factor analysis and clinical outcome data. The microarray has recently been extended with a 'satellite array' containing antibodies against cytokine, adhesion and apoptotic receptors that may be differentially expressed on subtypes of B-CLL.

In conclusion, there is close correlation between data obtained from the CD antibody microarray and traditional diagnostic methods across a wide range of leukaemias (Table I), but more data are needed for uncommon cases of leukaemia to better define expression profiles. The clustering of dot patterns (expression profiles, immunophenotypes, disease signatures) for acute leukaemias (Fig 6) and B-LPD (Fig 7) from PB and BMA validated the use of CD antibody microarrays for diagnosis. For the data from 796 subjects presented here, the overall levels of consensus were 93·9% (495/527) for PB and 97·6% (201/206) for BMA. The microarray provides a simple, unbiased procedure for immunophenotyping with far more information than flow cytometry without subjective gating. The extensive immunophenotypes obtained also have the potential to identify unusual CD antigens as targets for therapeutic antibodies. For flow cytometry, intracellular antigens, such as TdT, are also screened as markers to distinguish subtypes of leukaemia. With the extensive immunophenotype available from the microarray, intracellular antigens have not been required so far to distinguish subtypes except, perhaps for T-ALL from T-LPD. However, procedures have been developed to test cells captured on the microarray for expression of the intracellular antigens abl–bcr and TdT that will be the subject of a later report (unpublished observations).

The microarray has been used to quantify immunophenotypic changes induced by drugs on leukaemia and lymphoma cell lines (e.g. White *et al*, 2005) with the data obtained on different microarrays normalised on a maximum dot intensity of 255 (cf. Figs 3–5), or by using an internal standard such as CD44. The microarray is also being used for analysis of other diseases that affect sub-populations of leucocytes, for example, infection with human immunodeficiency virus (Woolfson *et al*, 2005). An extensive immunophenotype may enable systematic and unbiased sub-classification of AML and B-LPD based upon a single assay, and has the potential to detect new disease entities and prognostic groups.

Acknowledgements

We thank Asha Soosapilla (Symbion Health, Sydney, Australia), Sue Wong (ICPMR, Westmead Hospital, Sydney, Australia), Peter Chapple (Royal Melbourne Hospital, Melbourne, Australia) and Bobby Shelvin (MD Anderson Cancer Center, Houston, USA) for immunophenotyping samples using the CD antibody microarray, and providing clinical diagnoses and patient data. We also thank Dr Mark Lowdell (Royal Free Hospital, London, UK) for some frozen leukaemia samples. L.B., P.H., S.P.M., J.S.C. and R.I.C. have a financial interest in the company (Medsaic Pty Ltd) whose product was utilised in this study. L.B., P.H. and J.S.C. are employees of Medsaic Pty Ltd and one of the authors (R.I.C.) holds a patent related to the work. This study was supported in part by research funding from Medsaic Pty Ltd to R.I.C. DotScan™ is subject to intellectual property rights and information concerning its use may be obtained from Medsaic Pty Ltd, Suite 145, National Innovation Centre, Australian Technology Park, Garden Street, Eveleigh, NSW 1430, Australia. DotScan™ is a microarray of monoclonal CD antibodies and is dedicated to the memory of Mrs Lee Dixon.

References

Bain, B.J. (2003) *Leukemia Diagnosis*, 3rd edn. Blackwell Publishing, London.

Belov, L., de la Vega, O., dos Remedios, C., Mulligan, S.P. & Christopherson, R.I. (2001) Immunophenotyping of leukemias using a cluster of differentiation antibody microarray. *Cancer Research*, **61**, 4483–4489.

Belov, L., Huang, P., Barber, N., Mulligan, S.P. & Christopherson, R.I. (2003) Identification of repertoires of surface antigens on leukemias using an antibody microarray. *Proteomics*, **3**, 2147–2154.

Bene, M.C., Castoldi, G., Knapp, W., Ludwig, W.D., Matutes, E., Orfao, A. & van't Veer, M.B. (1995) Proposals for the immunological classification of acute leukemias: European Group for the Immunological Classification of Leukemias (EGIL). *Leukemia*, **9**, 1783–1786.

Bennett, J.M., Catovsky, D., Daniel, M.T., Flandrin, G., Galton, D.A., Gralnick, H.R. & Sultan, C. (1976) Proposals for the classification of the acute leukaemias: French–American–British (FAB) co-operative group. *British Journal of Haematology*, **33**, 451–458.

Bennett, J.M., Catovsky, D., Daniel, M.T., Flandrin, G., Galton, D.A., Gralnick, H.R. & Sultan, C. (1989) Proposals for the classification of chronic (mature) B and T lymphoid leukemias: French–American–British (FAB) Cooperative Group. *Journal of Clinical Pathology*, **42**, 567–584.

Bennett, J.M., Catovsky, D., Daniel, M.T., Flandrin, G., Galton, D.A., Gralnick, H.R. & Sultan, C. (1991) Proposal for the recognition of minimally differentiated acute myeloid leukaemia (AML-MO). *British Journal of Haematology*, **78**, 325–329.

Brouwer, R.E., Zwinderman, K.H., Kluin-Nelemans, H.C., van Luxemburg-Heijs, S.A., Willemze, R. & Falkenburg, J.H. (2000) Expression and induction of co-stimulatory and adhesion molecules on acute myeloid leukemic cells: implications for adoptive immunotherapy. *Experimental Hematology*, **28**, 161–168.

Brunning, R.D. (2003) Classification of acute leukemias. *Seminars in Diagnostic Pathology*, **20**, 142–153.

Casasnovas, R.O., Slimane, F.K., Garand, R., Faure, G.C., Campos, L., Deneys, V., Bernier, M., Falkenrodt, A., Lecalvez, G., Maynadie, M. & Bene, M.C. (2003) Immunological classification of acute myeloblastic leukemias: relevance to patient outcome. *Leukemia*, **17**, 515–527.

Dunphy, C.H., Polski, J.M., Evans, H.L. & Gardner, L.J. (2001) Evaluation of bone marrow specimens with acute myelogenous leukemia for CD34, CD15, CD117 and myeloperoxidase. *Archives of Pathology and Laboratory Medicine*, **125**, 1063–1069.

Dunphy, C.H., Orton, S.O. & Mantell, J. (2004) Relative contributions of enzyme cytochemistry and flow cytometric immunophenotyping to the evaluation of acute myeloid leukemias with a monocytic component and of flow cytometric immunophenotyping to the evaluation of absolute monocytoses. *American Journal of Clinical Pathology*, **122**, 865–874.

Exner, M., Thalhammer, R., Kapiotis, S., Mitterbauer, G., Knobl, P., Haas, O.A., Jager, U. & Schwarzinger, I. (2000) The "typical" immunophenotype of acute promyelocytic leukemia (APL-M3): does it prove true for the M3-variant? *Cytometry*, **42**, 106–109.

Ferrara, F., Di Noto, R., Annunziata, M., Copia, C., Lo Pardo, C., Boccuni, P., Sebastio, L. & Del Vecchio, L. (1998) Immunophenotypic analysis enables the correct prediction of t(8;21) in acute myeloid leukemia. *British Journal of Haematology*, **102**, 444–448.

Friedman, J. (1989) Regularised discriminant analysis. *Journal of the American Statistical Association*, **84**, 165–175.

Jaffe, E.S., Harris, N.L., Stein, H. & Vardiman, J.W. (2001) *World Health Organization Classification of Tumours: Pathology and Genetics: Tumours of Haematopoietic and Lymphoid Tissues*. IARC Press, Lyon.

Khalidi, H.S., Medeiros, L.J., Chang, K.L., Brynes, R.K., Slovak, M.L. & Arber, D.A. (1998) The immunophenotype of adult acute myeloid leukemia: high frequency of lymphoid antigen expression and comparision of immunophenotype, French–American–British classification, and karyotypic abnormalities. *American Journal of Clinical Pathology*, **109**, 211–220.

Khalidi, H.S., Chang, K.L., Medeiros, L.J., Brynes, R.K., Slovak, M.L., Murata-Collins, J.L. & Arber, D.A. (1999) Acute lymphoblastic leukaemia: Survey of immunophenotype, French–American–British classification, frequency of myeloid antigen expression, and karyotypic abnormalities in 210 pediatric and adult cases. *American Journal of Clinical Pathology*, **111**, 467–476.

Lacayo, N.J., Meshinchi, S., Kinnunen, P., Yu, R., Wang, Y., Stuber, C.M., Douglas, L., Wahab, R., Becton, D.L., Weinstein, H., Chang, M.N., Willman, C.L., Radich, J.P., Tibshirani, R., Ravindranath, Y., Sikic, B.I. & Dahl, G.V. (2004) Gene expression profiles at diagnosis in de novo childhood AML patients identify FLT3 mutations with good clinical outcomes. *Blood*, **104**, 2646–2654.

Legrand, O., Perrot, J.Y., Baudard, M., Cordier, A., Lautier, R., Simonin, G., Zittoun, R., Casadevall, N. & Marie, J.P. (2000) The immunophenotype of 177 adults with acute myeloid leukemia: proposal of a prognostic score. *Blood*, **96**, 870–877.

McCullagh, P. & Nelder, J.A. (1999) *Generalised Linear Models*, 2nd edn. Chapman and Hall/CRC, London.

Miyachi, H., Tanaka, Y., Gondo, K., Kawada, T., Kato, S., Sasao, T., Hotta, T., Oshima, S. & Ando, Y. (1999) Altered expression of CD45 isoforms in differentiation of acute myeloid leukemia. *American Journal of Hematology*, **62**, 159–164.

Munoz, L., Aventin, A., Villamor, N., Junca, J., Acebedo, G., Domingo, A., Rozman, M., Torres, J.P., Tormo, M. & Nomdedeu, J.F. (2003) Immunophenotypic findings in acute myeloid leukemia with FLT3 internal tandem duplication. *Haematologica*, **88**, 637–645.

Nguyen, A.N., Milam, J.D., Johnson, K.A. & Banez, E.I. (2000) A relational database for diagnosis of hematopoietic neoplasms using immunophenotyping by flow cytometry. *American Journal of Clinical Pathology*, **113**, 95–106.

Oscier, D., Fegan, C., Hillmen, P., Illidge, T., Johnson, S., Maguire, P., Matutes, E. & Milligan, D. (2004) Guidelines on the diagnosis and management of chronic lymphocytic leukaemia. *British Journal of Haematology*, **125**, 294–317.

Paietta, E., Goloubeva, O., Neuberg, D., Bennett, J.M., Gallagher, R., Racevskis, J., Dewald, G., Wiernik, P.H. & Tallman, M.S. (2004) A surrogate marker profile for PML/RARalpha expressing acute promyelocytic leukemia and the association of immunophenotypic markers with morphologic and molecular subtypes. *Cytometry*, **59B**, 1–9.

Paredes-Aguilera, R., Romero-Guzman, L., Lopez-Santiago, N. & Trejo, R.A. (2003) Biology, clinical, and hematologic features of acute megakaryoblastic leukaemia in children. *American Journal of Hematology*, **73**, 71–80.

R Development Core Team (2005) *A Language and Environment for Statistical Computing. R Foundation for Statistical Computing*, Vienna, Austria. ISBN 3-900051-07-0. http://www.R-project.org, accessed on 28 July.

Raspadori, D., Damiani, D., Lenoci, M., Rondelli, D., Testoni, N., Nardi, G., Sestigiani, C., Mariotti, C., Birtolo, S., Tozzi, M. & Lauria, F. (2001) CD56 antigenic expression in acute myeloid leukemia identifies patients with poor clinical prognosis. *Leukemia*, **15**, 1161–1164.

Re, F., Arpinati, M., Testoni, N., Ricci, P., Terragna, C., Preda, P., Ruggeri, D., Senese, B., Chirumbolo, G., Martelli, V., Urbini, B., Baccarani, M., Tura, S. & Rondelli, D. (2002) Expression of CD86 in acute myelogenous leukemia is a marker of dendritic/monocytic lineage. *Experimental Hematology*, **30**, 126–134.

Shaffer, A.L., Rosenwald, A. & Staudt, L.M. (2002) Lymphoid malignancies: the dark side of B-cell differentiation. *Nature Reviews Immunology*, **2**, 920–933.

Staudt, L.M. (2003) Molecular diagnosis of the hematologic cancers. *New England Journal of Medicine*, **348**, 1777–1785.

Thalhammer-Scherrer, R., Mitterbauer, G., Simonitsch, I., Jaeger, U., Lechner, K., Schneider, B., Fonatsch, C. & Schwarzinger, I. (2002) The immunophenotype of 325 adult acute leukemias: relationship to morphologic and molecular classification and proposal for a minimal screening program highly predictive for lineage discrimination. *American Journal of Clinical Pathology*, **117**, 380–389.

Venables, W.N. & Ripley, B.D. (2002) *Modern Applied Statistics with S*, 4 edn. pp. 331–338. Springer, Berlin.

White, S.L., Belov, L., Hodgkin, P.D. & Christopherson, R.I. (2005) Immunophenotypic changes induced on human HL60 leukaemia cells by 1α,25-dihydroxyvitamin D_3 and 12-O-tetradecanoyl phorbol-13-acetate. *Leukemia Research*, **29**, 1141–1151.

Woolfson, A., Stebbing, J., Tom, B., Stoner, K., Gilks, W., Kreil, D., Mulligan, S., Belov, L., Chrisp, J., Errington, W., Wildfire, A., Erber, W., Bower, M., Gazzard, B., Christopherson, R. & Scott, M. (2005) Conservation of unique CD cell surface mosaics in HIV infected individuals. *Blood*, **106**, 1003–1007.

Yatomi, Y., Yoneyama, A. & Nakahara, K. (2004) Usefulness of CD9 detection in the diagnosis of acute megakaryoblastic leukaemia. *European Journal of Haematology*, **72**, 229–230 (letter to the editor).

Supplementary material

The following supplementary material is available for this article online:

Appendix S1. Classification score details.

Table S1. Cell binding intensity mean.

Table S2. Standard error of the mean.

This material is available as part of the online article from http://www.blackwell-synergy.com

